ELSEVIER

Contents lists available at ScienceDirect

Journal of Computational Design and Engineering

journal homepage: www.elsevier.com

Improving the quality characteristics of abrasive water jet machining of marble material using multi-objective artificial bee colony algorithm

Padmakar J. Pawar*, Umesh S. Vidhate, Mangesh Y. Khalkar

Department of Production Engineering, K. K. Wagh Institute of Engineering Education and Research, Nashik, Savitribai Phule Pune University, Pune, Maharashtra, India

A R T I C L E   I N F O

Article history:
Received 28 June 2017
Received in revised form 12 November 2017
Accepted 11 December 2017
Available online xxx

Keywords:
Abrasive water jet machining
Kerf width
Kerf taper
Striation marks
Multi-objective artificial bee colony algorithm

A B S T R A C T

Although abrasive water jet machining has proved its capabilities for cutting marble material in a most economic and environment friendly manner, is facing serious issues related to dimensional inaccuracy and striation marks. This has put limit on its applications. Also, due to complex nature of abrasive water jet machining process, it is very difficult to control all three quality factors i.e. kerf taper, kerf width, striation marks simultaneously to achieve desired quality. This work therefore deals with multi-objective optimization considering three objectives as: minimization of kerf width, minimization of kerf taper, and maximization of depth of striation free surface in abrasive water jet machining process. The response surface modeling is used to establish the relation between various input parameters such as stand of distance, traverse speed, water pressure, and abrasive flow rate, with objectives mentioned above. Application of well-known meta-heuristics named artificial bee colony algorithm is extended to multi-objective optimization with posteriori approach by incorporating the concept of non-dominated sorting. Set of Pareto optimal solutions obtained by this proposed approach provides a ready reference for selecting most appropriate parameter setting on the machine with respect to objectives considered in this work.

1. Introduction

Abrasive water jet machining (AWJM) technology is one of the fastest growing nontraditional machining processes. It can machine almost any engineering material, irrespective of material properties. In comparison to traditional and most non-traditional machining technologies, AWJM exhibits better performance in the machining of difficult to machine materials such as ceramics, glass, marble and rocks. As the material thickness increases AWJM becomes the preferred cutting technique, especially where accuracy must be maintained.

The AWJM is used for making intricate decorative shapes or decorative profiles in marble material. Marble is a natural stone or rock resulting from metamorphism. Marble has number of applications in constructions, ceramics, paper, paint industries and decorative purposes. The diamond wire or saw cutters are conventionally used for cutting the marble material. During cutting the marble using diamond wire or saw cutter, the material grinds, rather than cut. Also various other drawbacks of conventional cutting of marble includes higher set up times, producing dust and noise, higher material wastage, unsuitability for profile cutting and cracking of material. Due to above mentioned issues encountered while conventional cutting of marble, attempts have been made for cutting of marble using nontraditional machining process such as ultrasonic machining, abrasive water jet machining (AWJM), laser beam machining (LBM) etc. However, although ultrasonic machining can be applied to non-conductive as well as brittle materials, it is a slow and time consuming process with very high tool wear rate (Hasan, Said, & Mustafa, 2008). Similarly, laser beam machining of marbles put constraint on the height of the work piece. Hence, AWJM has been claimed to be one of the most appropriate methods for cutting marbles due to its distinct advantages over the other cutting technologies, such as no thermal distortion of the work piece, high machining versatility to cut virtually any material, high flexibility to cut in any direction with small cutting forces, no risk of fire hazards no radiation emission, no tolerable noise levels, etc.

In spite of several advantages AWJM offers while machining the marble material, achieving desired quality of cutting is a challenge. The performance measures of the quality of cutting includes kerf width, kerf taper angle, and striations marks at bottom of machined surface. Several attempts have been made by the earlier researchers for modeling and optimization of abrasive water jet machining of different materials using various approaches such as genetic algorithm (Jain, Jain, & Deb, 2007; Srinivasu & Babu, 2008), simulated annealing (Zain, Haron, & Sharif, 2011a, 2011b), artificial bee colony algorithm (Yusup, Sarkheyli, Zain, Hashim, & Ithnin, 2013), teaching learning based optimization (Pawar & Rao, 2012), Multi-objective Jaya algorithm (Rao, Rai, & Balic, 2017), Taguchi method (Azmir & Ahsan, 2008, 2009; Babu & Muthukrishnan, 2015; Kechagias, Petropoulos, & Vaxevanidis, 2012; Selvan, Raju, Mohana, & Sachidananda, 2012), artificial neural network (Caydas & Hascalik, 2008), response surface methodology (Babu & Muthukrishnan, 2017; Irina Wong, Azmi, Lee1, & Mansor, 2016; Jagadish & Ray, 2016; Liu et al., 2014), fuzzy logic (Jegaraj & Babu, 2007; Vundavilli, Parappagoudar, Kodali, & Benguluri, 2012), bio-geography algo-

* Corresponding author.
Email addresses: pjpawar1@rediffmail.com (P.J. Pawar); umeshvidhate30@gmail.com (U.S. Vidhate); mykhalkar@kkwagh.edu.in (M.Y. Khalkar)

https://doi.org/10.1016/j.jcde.2017.12.002
2288-4300/© 2017.

rithm (Rajkamal & Singh, 2017) and sequential approximation optimization (Yue et al., 2014).

It is revealed from literature review that most of the attempts made by earlier researchers are based on single objective optimization of AWJM process. Although few attempts have been made for multi-objective optimization of AWJM process, are mostly based on priori approach. In priori approach of multi-objective optimization, the weights of the objectives are to be decided by process engineers before optimization, which is very difficult task as it requires comprehensive knowledge of the process. Also with priori approach single optimum solution is obtained which is prone to change with change in weights of the objectives. Artificial bee colony algorithm developed by Karaboga and Basturk (2008) has been proved to be one of the most powerful and robust algorithms for single objective optimization of several real life applications. Few recent applications of artificial bee colony algorithm in the field of advanced machining processes includes parametric Optimization of Nd: YAG Laser Beam Machining Process (Mukherjee, Goswami, & Shankar, 2013), optimization of wire electric discharge machining (Rao & Pawar, 2009), optimization of electrochemical machining (Sumanta & Chakraborty, 2011), etc. Few attempts also have been made recently for multi-objective optimization using artificial bee colony algorithm (Luo et al., 2017; Wang et al., 2015). In this work an attempt is made to extend the application of artificial bee colony algorithm to multi-objective optimization through incorporating the concept of non-dominated sorting (Deb, 2005). The multi-objective artificial bee colony algorithm is discussed in the next section.

2. Multi-objective artificial bee colony algorithm

Artificial bee colony algorithm is developed to model the intelligent behaviors of honeybee swarms (Karaboga & Basturk, 2008). The honeybee swarms consists of three essential components: food sources, employed foragers and unemployed foragers, and defines two leading modes of the behavior: recruitment to a nectar source and abandonment of a source.

(i) *Food sources:* the value of a food source depends on many factors, such as its proximity to the nest, richness or concentration of energy and the ease of extracting this energy. For the simplicity, the ‘‘profitability’’ of a food source can be represented with a single quantity
(ii) *Employed foragers:* they are associated with a particular food source, which they are currently exploiting or are ‘‘employed’’ at. They carry with them information about this particular source, its distance and direction from the nest and the profitability of the source and share this information with a certain probability.
(iii) *Unemployed foragers:* they are looking for a food source to exploit. There are two types of unemployed foragers scouts searching the environment surrounding the nest for new food sources and onlookers waiting in the nest and finding a food source through the information shared by employed foragers.

The exchange of information among bees is the most important occurrence in the formation of collective knowledge. While examining the entire hive, it is possible to distinguish some parts that commonly exist in all hives. The most important part of the hive with respect to exchanging information is the dancing area. Communication among bees occurs through waggle dance. Employed foragers share their information with a probability, which is proportional to the profitability of the food source, and the sharing of this information through waggle dancing is longer in duration. Hence, the recruitment is proportional to profitability of a food source.

The performance of artificial bee colony (ABC) algorithm in terms of convergence rate and accuracy of the solution is found superior over other non-traditional algorithms in many recent applications. ABC algorithm combines both, the stochastic selection scheme carried out by onlooker bees, and greedy selection scheme used by onlookers and employed bees to update the source position. Also the neighbor source production mechanism in ABC is similar to the mutation process, which is self-adapting. The random selection process carried out by the scout bees maintains diversity in the solution. The ABC algorithm is thus flexible, simple to use and robust optimization algorithm, which can be used effectively in the optimization of multi-modal and multi-variable problems. To extend the application of ABC algorithm for multi-objective optimization with posteriori approach, concept of non-dominated sorting is incorporated in this work as discussed through following steps.

Step 1: Parameter selection

Algorithm specific parameters such as population size i.e. number of food sources (equal to number of employed bees), number of onlooker bees, number of scout bees (5–30% of the colony size) are to be determined.

Step 2: Calculate the nectar amount for each food source

The nectar amount represents the actual fitness value of the solution.

Step 3: Non-dominate sorting of solutions

In first sorting, each solution is selected and checked whether it satisfies the rules given by Eq. (1) with respect to any other solution in the population

$$\text{Obj.1[i]} < \text{Obj.1[j] and Obj.2[i]} < \text{obj.2[j]}, \quad i \neq j \tag{1}$$

If the rules are satisfied for any one of the remaining solutions, then the selected solution is marked as dominated. Otherwise, the selected solution is marked as non-dominated. All the non-dominated solutions in the first sorting are ranked 1. Eq. (1) is then again applied to remaining (dominated) solutions from the first sorting and non-dominated solutions identified in this second sorting are ranked 2. The procedure is repeated until all the solutions are ranked. The subpopulation with rank 1, referred to as first front set, is assigned a dummy fitness value.

Step 4: Determine normalized Euclidean distance of each solution

Then, the normalized Euclidean distance of each solution is calculated with respect to all other solutions within this first front set using the formula

$$d_{ij} = \sqrt{\sum \frac{(x_s^i - x_s^j)}{x_s^{\max} - x_s^{\min}}} \tag{2}$$

where x_s the value of sth decision variable and i, j are solution numbers. $x_s^{\max}$ and $x_s^{\min}$ are upper and lower limits of the sth decision variable respectively.

Step 5: Determine niche count of the solution

A niche count (nc_i) provides an estimate of the extent of crowding near a solution and is calculated using the equation

$$nc_i = \sum sh(d_{ij}) \tag{3}$$

where $Sh(d_{ij})$ is the sharing function values of all the first front solutions as given by equation:

$$Sh(d_{ij}) = \left\{1 - \left(\frac{d_{ij}}{\sigma_{share}}\right)^2\right\} \quad if\ d_{ij}<\sigma_{share}$$
$$= 0 \quad \text{otherwise} \tag{4}$$

where σ_{share} is the maximum distance allowed between any two solutions to become members of a niche. The σ_{share} value in this equation is to be chosen appropriately.

Step 6: Determine the shared fitness values of the solutions

The shared fitness values (F) are then calculated by dividing the dummy fitness values by the niche count, which is given by Eq. (5).

$$Shared\ fitness\ (F_i) = Dummy\ fitness\ (f)/nc_i \tag{5}$$

After calculating the shared fitness values for the first front, a smaller value is subtracted from the minimum shared fitness value in this front and resultant value is given as the dummy fitness value (F_2) for all the next front (rank 2) solutions and the steps are repeated. This procedure is continued till the shared fitness values are calculated for all fronts.

Step 7: Determine the probabilities by using the shared fitness values evaluated in step 6

If the shared fitness of a food source "$_i$" is F_i, then the probability (P_i) of choosing this food source by an onlooker bee is expressed as:

$$P_i = \frac{\sum_{k=1}^{R}(1/f_k)^{-1}}{f_i} \tag{6}$$

where R is number of food sources.

Step 8: Calculate the number of onlooker bees, which will be sent to food sources

The number of onlookers bees (N) sent to food source "θ_i" is calculated as:

$$N = P_i \times m. \tag{7}$$

where 'm' is the total number of onlooker bees.

Step 9: Determine new position of each onlooker bee

After watching the dances of employed bees, an onlooker bee goes to the region of food source "θ_i" with the probability P_i. The position of the selected neighbor food source is obtained as below:

$$\theta_i(c+1) = \theta_i(c) \pm \phi_i(c) \tag{8}$$

where "c" is number of generation. $\phi_i(c)$ is a randomly produced step to find a food source with a more nectar around 'θ_i'. Each food source is then updated if better position is obtained by onlooker assigned to that food source.

Step 10: Evaluate the best solution

Position of the best onlooker bee is identified for each food source. The global best of the honeybee swarm in each generation is obtained and it may replace the global best at previous generation if it has better fitness value.

Step 11: Update the scout bee

The worst employed bees, as many as the number of scout bees in the population, are respectively compared with the scout solutions. If the scout solution is better than employed solution, employed solution is replaced with scout solution. Else employed solution is transferred to the next generation without any change.

A flowchart of multi-objective artificial bee colony algorithm based on non-dominated sorting concept is shown in Fig. 1.

3. Application example

An application example considered in this work is a profile cutting in rectangular slab of marble material using abrasive water jet machining process. The details of experimental set up used for data collection are given below:

- Machine type:5 axis SL-V E50V2 abrasive water jet machine
- Make: TECHNI water jet systems
- Workpiece specification: Rectangular slab of 100 mm × 7 mm × 18 mm
- Types of abrasives: Garnet
- Abrasive size: 80 mesh
- Jet impact angle: 90°
- Orifice diameter: 0.25 mm
- Nozzle diameter: 0.762 mm
- Nozzle length: 76.2 mm
- Water flow rate: 2.3 L/min
- Number of passes: 1.

As mentioned earlier, the main issues related to profile cutting in marble material are higher kerf width, higher kerf taper angle and large striations marks at bottom of cutting surface as demonstrated by Fig. 2. Fig. 2(a) shows the work piece and (b) shows the slug images after machining.

To overcome all these issues, the objectives set for multi objective optimization are (1) minimizing the kerf width (W), (2) minimizing the kerf taper angle ($\theta°$) and (3) maximizing the depth of striation free surface (D). Workpiece details with kerf geometry of an abrasive water jet cut are shown in Fig. 3.

Although several variables plays an important role in AWJM performance, keeping in view the specific objectives considered in this work the process variables namely standoff distance (S), traverse speed (V), water jet pressure (P), and abrasive flow rate (A_f) are selected for this study.

Using response surface modeling approach, an experiment is designed with 2^k (where k is number of process parameters in this case $k=4$) factorial with central composite-second order rotatable design is used. This consist of number of corner points = 16, number of axial points = 8, and a center point at zero level = 4. The axial points are located in a coded test condition space through parameter 'α'. For the design to remain rotatable, 'α' is determined as $(2^k)^{1/4}=2$. Thus the coded level for the axial points is at 2. The operating ranges for process parameters and their coded values shown in Table 1.

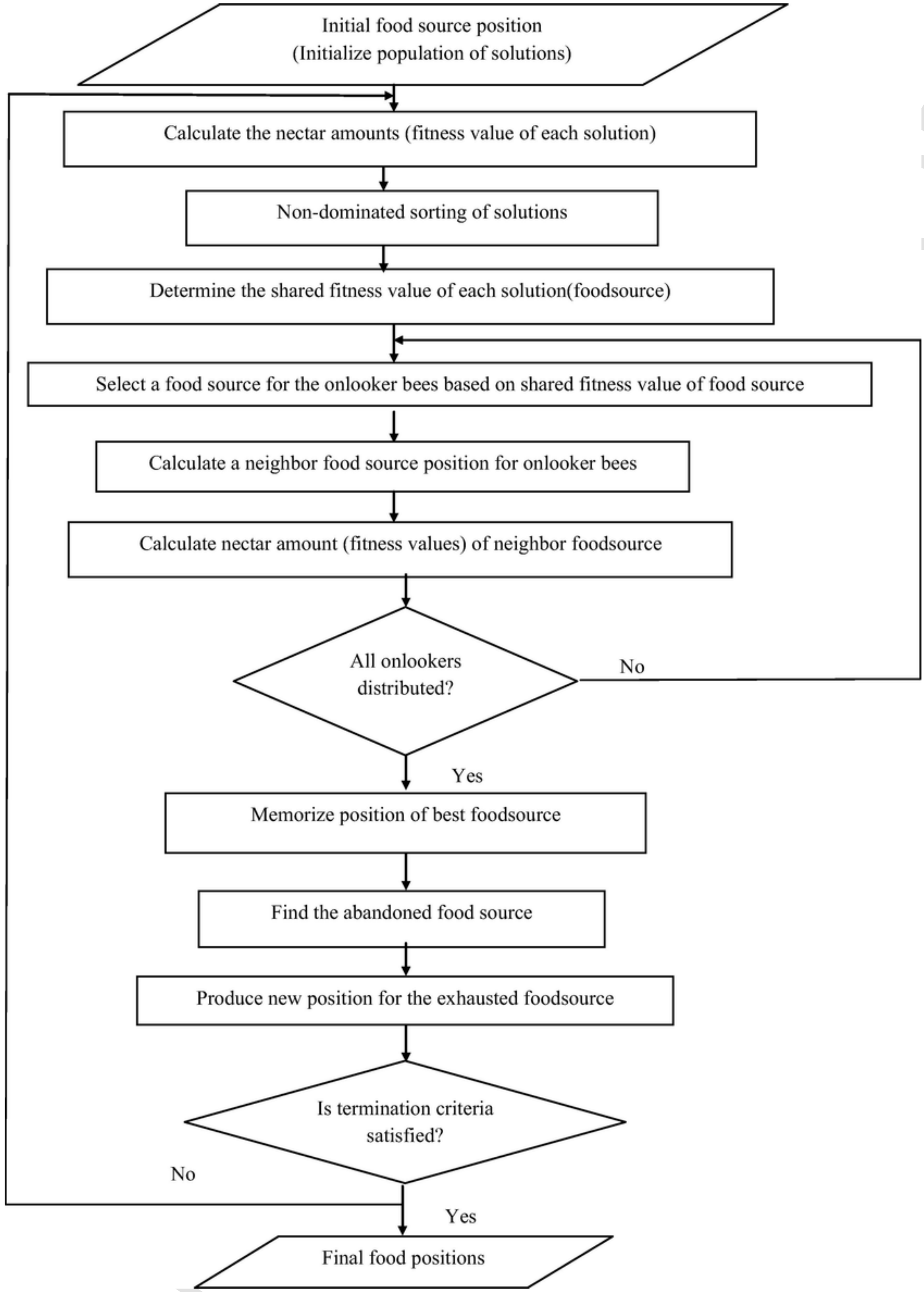

Fig. 1. Flowchart of multi-objective artificial bee colony algorithm based on non-dominated sorting concept.

In this work the performance measures i.e. kerf width (W), kerf taper angle ($\theta°$) and depth of striation free surface (D) are considered. The experimental data have been collected for above parameters and measured using calibrated measuring devices. The kerf width is obtained by evaluating the difference of internal diameter of the plate and the diameter of the cut out part as shown in Fig. 4.

Kerf taper angle have been measured using coordinate measuring machine. The depth of striation is measured using digital Vernier-Caliper. Data collected experimentally are presented in Table 2.

To study the effect of process parameters i.e. V, P, A_f, S on performance measures i.e. kerf width (W), kerf taper angle ($\theta°$) and depth of striation free surface (D) a second order polynomial response is fit-

(a) (b)

Fig. 2. (a) Workpiece. (b) Slug after machining.

ted into following Eq. (9).

$$Y = b_0 + \sum_{i=1}^{k} b_i x_i + \sum_{i=1}^{k} b_{ii} x_i^2 + \sum_{j>1}^{k} b_{ij} x_i x_j \tag{9}$$

where 'y' is the response and the x_i (1, 2, …, k) are coded levels of k quantitative variables. The coefficient b_0 is the free term, the coefficient b_i are the linear terms, the coefficient b_{ii} are the quadratic terms and the coefficient b_{ij} are the interaction terms.

The mathematical models are derived for kerf width (W), kerf taper angle ($\theta°$) and depth of striation free surface (D) based on the observation collected by determining the coefficients b_0, b_{ii}, b_{ij} using least square technique. Multiple regression analysis tool of Microsoft Excel 2010 is implemented to get following equations.

$$\begin{aligned} W = {} & 1.1435125 + 0.00804167x_1 - 0.017858x_2 - 0.049429x \\ & -0.02795x_2^2 + 0.010275x_3^2 - 0.0148625x_4^2 + 0.0200812 \\ & -0.04360625x_1 \cdot x_4 + 0.03755x_2 \cdot x_3 + 0.01001875x \end{aligned}$$

$$\begin{aligned} \theta = {} & 0.9580575 + 0.0263904x_1 + 0.0732204x_2 + 0.467849x_3 \\ & -0.039688438x_2^2 + 0.03312406x_3^2 + 0.122430313x_4^2 + 0.2299 \\ & +0.057566875x_1 \cdot x_4 + 0.052045625x_2 \cdot x_3 - 0.156149375 \end{aligned}$$

$$\begin{aligned} D = {} & 6.925 + 1.2075x_1 + 1.10916667x_2 - 0.1975x_3 + 0.07x_4 \\ & +0.77x_3^2 + 0.24625x_4^2 + 0.08625x_1 \cdot x_2 + 1.33875x_1 \cdot x \\ & +2.22375x_2 \cdot x_3 + 0.67375x_2 \cdot x_4 + 2.57625 \end{aligned}$$

4. Multi objective optimization using non dominated sorting based artificial bee colony algorithm

Now, to demonstrate and validate the non-dominated sorting based artificial bee colony algorithm for parameter optimization of wire electric discharge machining for the application example discussed in section 3, following multi-objective optimization model is formulated:

Objective 1: Minimize kerf width (W) as given by Eq. (10)

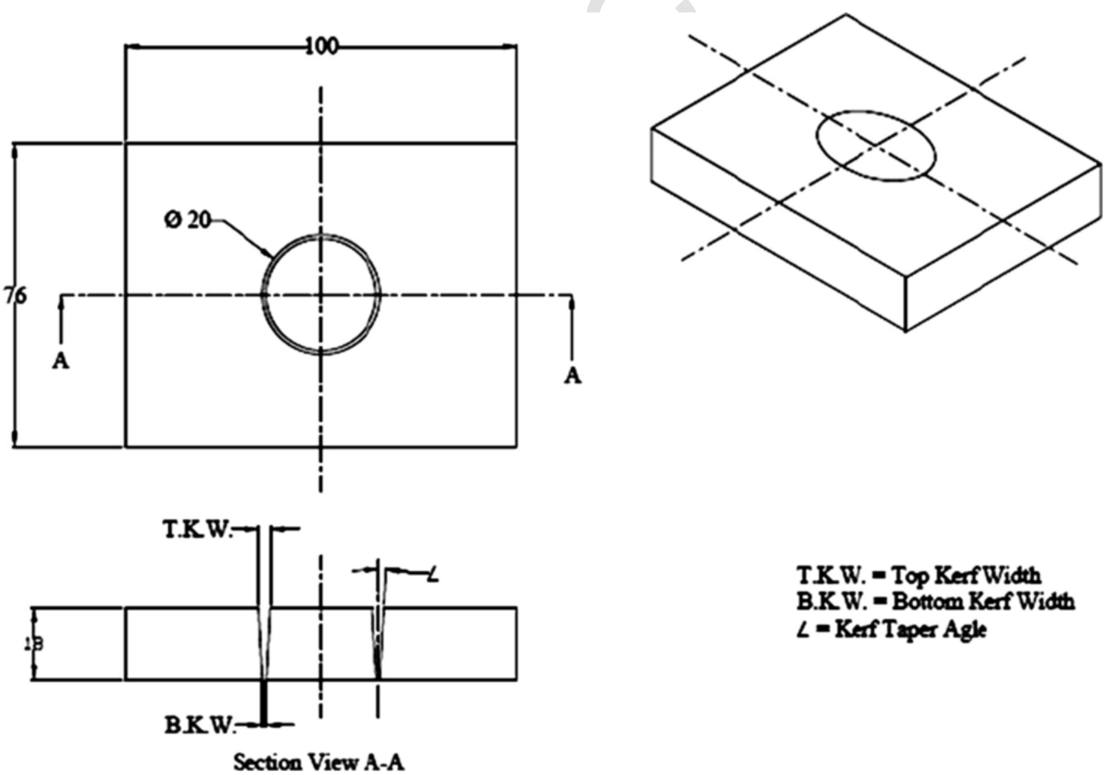

Fig. 3. Workpiece details and kerf geometry of an abrasive water jet cut.

Table 1
Coded values of process parameters.

Parameters	Unit	Coded levels				
		−2	−1	0	1	2
Stand Off Distance (S), (x_1)	mm	0.5	1	1.5	2	2.5
Traverse Speed (V), (x_2)	mm/min	50	72.5	95	117.5	140
Water Jet Pressure (P), (x_3)	MPa	138	190	242	294	346
Abrasive Flow Rate (A_f), (x_4)	g/s	200	375	550	725	900

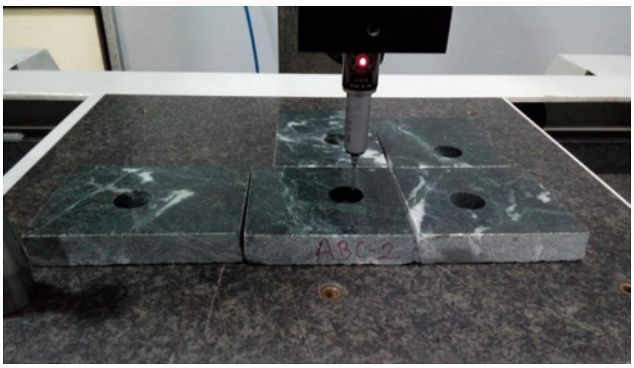

Fig. 4. Internal diameter measurement to find kerf width.

Table 2
Experimental data collection matrix.

Sr. No.	(S) mm	(V) mm/min	(P) MPa	(A_f) g/s	Kerf Width (W) mm	Kerf Taper Angle (θ) °	Depth of striation free surface (D) mm
1	−1	−1	−1	−1	1.29	0.40	15.00
2	1	−1	−1	−1	1.20	0.73	12.50
3	−1	1	−1	−1	1.10	1.21	9.42
4	1	1	−1	−1	1.25	0.00	9.90
5	−1	−1	1	−1	1.10	3.10	8.10
6	1	−1	1	−1	1.11	1.18	6.30
7	−1	1	1	−1	0.91	1.68	3.20
8	1	1	1	−1	1.22	5.31	0.00
9	−1	−1	−1	1	1.24	0.00	5.20
10	1	−1	−1	1	1.18	0.87	11.10
11	−1	1	−1	1	1.00	0.90	4.00
12	1	1	−1	1	1.12	1.02	6.70
13	−1	−1	1	1	1.03	0.99	3.00
14	1	−1	1	1	1.06	1.17	0.00
15	−1	1	1	1	1.36	0.40	0.00
16	1	1	1	1	0.98	1.00	0.00
17	−2	0	0	0	1.14	1.17	8.60
18	2	0	0	0	1.19	0.19	5.80
19	0	−2	0	0	1.05	0.81	8.70
20	0	2	0	0	0.97	0.15	0.00
21	0	0	−2	0	1.30	0.39	15.10
22	0	0	2	0	1.02	1.15	3.34
23	0	0	0	−2	1.03	0.86	7.10
24	0	0	0	2	1.09	1.40	7.15
25	0	0	0	0	1.10	1.59	10.10
26	0	0	0	0	1.10	0.53	6.00
27	0	0	0	0	1.18	0.86	4.60
28	0	0	0	0	1.19	0.85	7.00

Objective 2: Minimization of kerf taper angle (θ) as given by Eq. (11).
Objective 3: Maximization of depth of striation free surface (D) as given by Eq. (12).

For demonstration purpose first 5 solutions are considered for all steps. The steps of the multi-objective optimization using non-dominated sorting based artificial bee colony algorithm are as discussed below:

Step 1: Parameter selection:

Following algorithm specific parameters are considered in this work.

- Number of food sources: 20
- Number of onlooker bees: 50
- Number of scout bees: 1

Step 2: Evaluate quality of each food source

Quality of each food source is obtained by evaluating objective functions values as shown in Table 3.

Step 3: Non-dominated sorting of solutions

Non-dominated sorting of all solution is done by applying criteria mentioned in Eq. (1). All solutions are ranked based on the level at which they attain non-dominated status. The ranking of solution is shown in Table 4.

Step 4: Determine normalized Euclidean distance of each solution

The normalized Euclidean distance of each solution from every other solution is computed by using Eq. (2) and is presented in Table 5.

Step 5: Determine niche count of the solution

Sharing function values shown in Table 6 are obtained by using Eq. (4). Niche count for solutions 1 to 5 is obtained as 5.302, 7.822, 5.648, 9.898, and 7.570 respectively.

Step 6: Determine the shared fitness values of the solutions

Considering dummy fitness value for rank 1 solution as 50, the shared fitness value for solutions is computed by applying Eq. (5).

Table 3
Nectar amount for each food source.

Food source No.	S (mm)	V (mm/min.)	P (MPa)	A_f (g/s)	W (mm)	θ°	D (mm)
1	1.87	71.22	325.82	254.11	0.97	3.44	2.95
2	0.84	89.85	164.61	385.93	1.23	0.36	13.32
3	0.79	100.12	142.11	315.17	1.19	0.10	14.42
4	2.16	120.38	259.75	623.01	1.12	1.44	1.97
5	2.41	87.55	271.91	897.67	0.94	1.00	3.50

Table 4
Non-dominated sorting of solutions.

Solution No.	(W) mm	(θ) °	(D) mm	Rank
1	0.97	3.44	2.95	2
2	1.23	0.36	13.32	2
3	1.19	0.10	14.42	1
4	1.12	1.44	1.97	3
5	0.94	1.00	3.50	1

Table 5
Normalized Euclidean distances.

Sol. No.	1	2	3	4	5
1	0.000	0.971	1.088	0.835	1.009
2	0.971	0.000	0.189	0.934	1.189
3	1.088	0.189	0.000	1.017	1.326
4	0.835	0.934	1.017	0.000	0.553
5	1.009	1.189	1.326	0.553	0.000

Table 6
Sharing function values.

Solutions	Sharing function values				
	1	2	3	4	5
1	1.000	0.056	0.000	0.302	0.000
2	0.056	1.000	0.964	0.128	0.000
3	0.000	0.964	1.000	0.000	0.000
4	0.302	0.128	0.000	1.000	0.694
5	0.000	0.000	0.000	0.694	1.000

The dummy fitness value for second rank solutions is obtained to ensure that it should be less than rank 1 solution with minimum shared fitness value. In similar way the dummy fitness values of subsequent ranks 2, 3, and 4 are obtained as 3.586, 0.281, and 0.019 respectively. The shared fitness values for solutions 1 to 5 are 0.676, 0.458, 8.853, 0.028, and 6.605 respectively.

Step 7: Determine the probabilities based on the shared fitness values evaluated in step 6

The probability (P_i) with which the onlooker bee is assigned to employed bee is obtained based on the shared fitness is obtained using Eq. (6). Values of P_i for solutions 1 to 5 are 0.012, 0.008, 0.157, 0.001, and 0.117 respectively.

Step 8: Calculate the number of onlooker bees, which will be sent to food sources

The number of onlooker bees sent to an employed bee (N) obtained using Eq. (7) for solutions 1 to 5 are 1, 0, 8, 0, and 6 respectively.

Step 9: Determine new position of each onlooker bee

Each employed bee is updated (for N times) using Eq. (8) to obtain positions of onlooker bees assigned to employed bees/food sources 1, 3, and 5. As mentioned in step 8, one onlooker bee is assigned to food source1, eight onlooker bees are assigned to food source3 and six onlooker bees are assigned to food source5. The positions of these onlooker bees are obtained as mentioned in Table 7.

The positions of onlooker bees for each food source are then compared with the position of the employed bee assigned to that food source. The comparison is made based on the combined objective function obtained considering equal weights to all objective functions. The combined objective function (to be minimized) is then evaluated as:

Table 7
Positions of onlooker bees.

Food source	Positions of onlooker bee assigned to food source	(W) mm	(θ) °	(D) mm	Z
1	1. (1.89, 74.70, 322.14, 312.24)	1.00	3.02	2.66	101.14*
3	1. (0.77, 94.85, 158.32, 281.74)	1.18	0.18	14.79	6.22
	2. (0.65, 98.07, 141.67, 622.35)	1.25	0.87	8.77	29.34
	3. (0.81, 111.67, 144.14, 263.27)	1.09	0.21	13.47	7.25*
	4. (0.53, 99.59, 176.05, 325.33)	1.11	0.57	12.58	19.31
	5. (0.74, 102.37, 161.56, 294.56)	1.13	0.22	13.48	7.56
	6. (0.70, 101.41, 175.44, 352.96)	1.13	0.46	12.05	15.75
	7. (1.04, 94.87, 142.11, 287.93)	1.25	0.30	15.84	10.15
	8. (0.80, 101.75, 181.46, 559.45)	1.18	0.60	8.71	20.44
5	1. (1.93, 80.77, 271.91, 895.20)	0.98	0.82	2.89	27.62
	2. (2.35, 75.68, 274.64, 897.87)	0.90	0.84	3.05	28.39
	3. (2.47, 106.42, 213.00, 469.85)	1.27	0.88	8.06	29.82
	4. (2.43, 98.71, 215.44, 897.67)	0.98	1.40	8.38	47.09
	5. (2.21, 83.34, 309.98, 897.67)	0.94	0.68	0.27	23.02*
	6. (2.43, 91.73, 242.88, 900.00)	0.96	1.20	6.05	40.37

* Best onlooker bee position among onlooker bees assigned to particular food source.

$$\min Z = \frac{W}{W^*} + \frac{\theta}{\theta^*} - \frac{D}{D^*} \tag{13}$$

where W^*, θ^*, D^* and are threshold values of kerf width, kerf taper angle, and depth of striation free surface respectively. The values of combined objective functions for employed and onlooker bees using Eq. (13) are shown in Table 7.

It is observed that combined objective function value (=101.14) of best onlooker bee for food source 1 is better than that of employed bee 1 (=114.87), and also combined objective function value of best onlooker bee for food source 5 (=23.02) is better than that of employed bee 5 (=33.71). Hence the positions of food source1 and 5 are updated. For food source3, combined objective function value of employed bee (=3.58) is better than that of (=6.22) best onlooker bee position hence the position of the employed bee is retained. Table 8 shows the new set of first five solutions.

This process maintains elitism as best among new solutions is compared with old solution and the one which is superior gets selected.

Step 10: Evaluate the best solution

The global best of the honeybee swarm is (0.79, 100.12, 142.11, 315.17) with $W = 1.19$ mm, $\theta = 0.10°$ and $D = 14.42$ mm respectively.

Step 11: Update the scout bee

Since number of scout bee is one, a random solution is generated as (2.30, 66.90, 236.28, 64.16) with $Z = 30.17$. The worst of the updated solution is (1.89, 74.70, 322.14. 312.24) with $Z = 101.14$. As the randomly generated (scout) solution is better than the worst solution, the worst solution will be replaced by scout solution.

Step 12: Obtain the set of Pareto-optimal solution

The set of Pareto optimal solutions as shown in Table 9 and The Pareto front is as shown in Fig. 5.

This process maintains elitism as best among new solutions is compared with old solution and the one which is superior gets selected. As shown in Table 9, the solution number 10 provides the best possible values for both kerf taper angle (0.001°) and depth of striation free surface (17.028 mm) and hence is chosen to emphasize the points of agreement and disagreement with results reported by earlier researchers (Karakurt, Aydin, & Aydiner, 2011; Orbabic & Junkar, 2008) as summarized in Table 10.

It is thus observed from Table 10, that the results of solution number 10 from the set of Pareto optimal solutions obtained in this work are in good agreement with those reported by earlier researchers. However, it is to be noted that the other solutions in Table 9 may not be in exact agreement with those reported by earlier researchers. This is due to the fact the results of optimization obtained by earlier researchers (Jain et al., 2007; Karakurt et al., 2011; Mali & Pawar, 2017; Orbabic & Junkar, 2008; [33]) are mainly based on single ob-

Table 8
Set of updated food sources.

Food source No.	S (mm)	V (mm/min.)	P (MPa)	A_f (g/s)	W (mm)	$\theta°$	D (mm)
1	1.89	74.70	322.14	312.24	1.00	3.02	2.66
2	0.84	89.85	164.61	385.93	1.23	0.36	13.32
3	0.79	100.12	142.11	315.17	1.19	0.10	14.42
4	2.16	120.38	259.75	623.01	1.12	1.44	1.97
5	2.21	83.34	309.98	897.67	0.94	0.68	0.27

Table 9
Set of Pareto optimal solutions.

Solution Number	(S) mm	(V) mm/min.	(P) MPa	(A_f) g/s.	Kerf Width (W) mm	Kerf Taper Angle (θ) °	Depth of striation free surface (D) mm
1	2.50	62.02	189.57	670.38	1.145	0.005	11.794
2	2.12	84.00	181.58	490.62	1.293	0.001	13.024
3	1.71	50.00	344.76	900.00	0.799	0.062	0.000
4	2.15	75.79	198.31	448.73	1.276	0.001	12.121
5	0.61	140.00	240.21	578.05	0.958	0.007	0.329
6	2.34	77.38	163.82	614.45	1.274	0.003	14.542
7	0.99	84.07	157.17	285.70	1.255	0.015	15.991
8	2.02	50.00	223.98	208.49	1.186	0.045	12.370
9	0.96	91.99	153.43	303.37	1.229	0.005	15.171
10	0.68	77.79	138.00	281.43	1.299	0.001	17.028
11	0.77	140.00	200.06	900.00	0.985	0.004	0.000
12	2.50	50.00	343.75	900.00	0.623	0.079	0.000
13	2.48	50.00	186.29	722.95	1.059	0.014	10.785
14	2.50	50.00	344.76	900.00	0.622	0.075	0.000

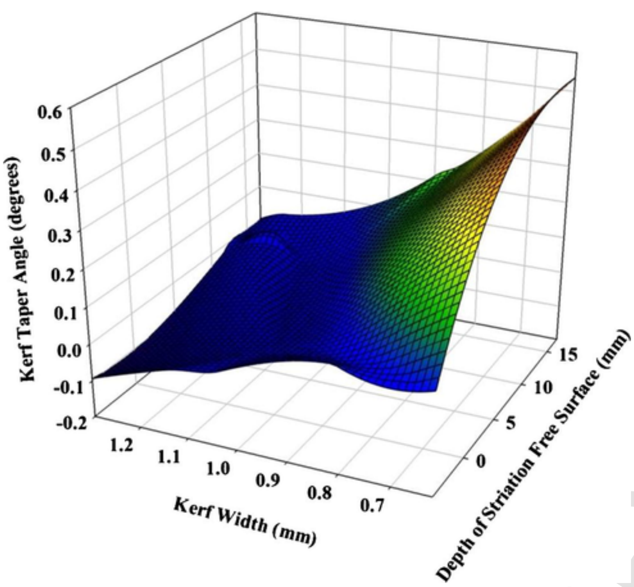

Fig. 5. Pareto front for three objective functions.

jective optimization, whereas those obtained in this work are for multi-objective optimization and hence provides the compromised best values of the process parameters.

Although the parameters ranges available on machine are very wide, this study reveals that parameter values in some specific ranges are only effective to achieve better process performance of wire electric discharge machining process with respect to the objectives considered. The most effective ranges of process variables to ensure best performance with respect to both objectives considered in this work are provided by value path plot as shown in Fig. 6.

Table 10
Process parameter effect matrix.

	For minimum kerf width	For minimum kerf taper angle	For maximum depth of striation free surface	Results of solution 10 in set of Pareto optimal solution
Stand Off Distance	Should be Less (Karakurt et al., 2011; Mali & Pawar, 2017)	Should be Less (Mali & Pawar, 2017)	Should be Less (Mali & Pawar, 2017)	0.68 mm; very close to lower bound
Traverse speed	Should be High (Karakurt et al., 2011), Should be moderate (Mali & Pawar, 2017)	Should be Low (Mali & Pawar, 2017)	Should be Low (Mali & Pawar, 2017; Orbabic & Junkar, 2008)	77.79 mm; moderately close to lower bound
Water pressure	Should be low up to threshold value and should be high above threshold value (Karakurt et al., 2011), Should be low (Mali & Pawar, 2017)	Lower or upper bound (Mali & Pawar, 2017)	Should be Low (Mali & Pawar, 2017; Orbabic & Junkar, 2008)	138 MPa; Lower bound value
Abrasive flow rate	Should be Low (Karakurt et al., 2011; Mali & Pawar, 2017)	Should be Low (Mali & Pawar, 2017)	Should be moderate (Mali & Pawar, 2017)	281.43 g/s; moderately close to lower bound

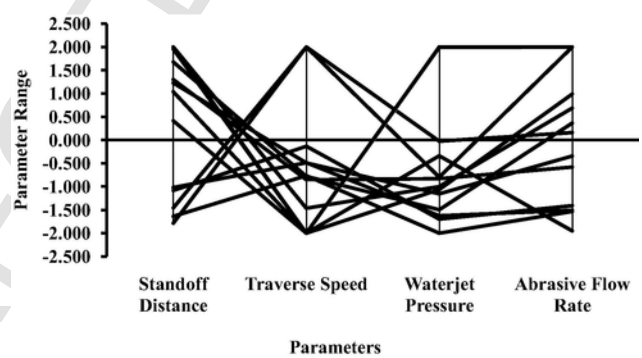

Fig. 6. Value path plot.

Few solutions from set of Pareto optimal solutions (solution no. 2, solution no. 8, and solution no. 13 from Table 9) are validated experimentally and the results are as shown in Table 11.

It is observed from Table 11 that average deviations of the predicted values from experimentally obtained values of kerf width, kerf taper angle and depth of striation free surface are 0.191 mm, 0.436°, and 2.263 mm respectively. Slug after machining for optimum solution 2 (from set of Pareto optimal solutions provided in Table 9) is shown in Fig. 7.

Table 11
Experimental validations of optimum solutions obtained using proposed multi-objective artificial bee colony algorithm.

Solution No.	Kerf Width (W) mm			Kerf Taper Angle (θ)°			Depth of striation free surface (D) mm		
	Predicted	Experi-mental	δ (mm)	Predicted	Experi-mental	δ (°)	Predicted	Experi-mental	δ (mm)
2	1.293	1.350	0.057	0.001	0.429	0.428	13.024	14.100	1.076
8	1.186	1.354	0.168	0.045	0.624	0.579	12.370	15.900	3.530
13	1.059	1.409	0.350	0.014	0.315	0.301	10.785	8.600	2.185

δ: Absolute deviation.

Fig. 7. Slug after machining for solution No. 2 from set of Pareto optimal solutions provided in Table 9.

5. Conclusions

- A set of 14 non-dominated solutions is obtained using proposed multi-objective optimization approach. This provides ready reference to process engineers to set best operating parameters on machines as per his/her requirements.
- It is observed that with optimized set of parameters, the best possible depth of striation free surface is 17.028 mm, which means almost entire surface is striation free. Also best possible values of kerf width and kerf taper angle are very low, 0.622 mm and 0.001° respectively. Thus with optimized set of parameters near net shape machining of marble material is possible, eliminating the need for further finishing operations.
- It is also revealed from value path plot that from kerf taper, kerf width, and depth of striation free surface point of view most effective ranges of process parameters are: stand-off distance: 0.75–1 mm and 1.75–2.5 mm, traverse speed: 50–95 mm/min, water jet pressure: 140–230 MPa, Abrasive flow rate: 200–900 g/s.
- Average combined objective function value (*Z*) of set of non-dominated solutions obtained by using proposed multi-objective ABC algorithm is 1.23 while that of initial data set obtained experimentally is 36.50. It can be thus inferred that the results obtained by using proposed multi-objective ABC algorithm shows an overall improvement of about 96.31% over those obtained by initial experimental data set.
- The results of optimization are validated experimentally and are in good agreement as indicated by low values of average absolute deviation of 0.191 mm, 0.436°, and 2.263 mm for kerf width, kerf taper angle and depth of striation free surface respectively. The proposed approach of multi-objective optimization has thus proved its effectiveness to the application presented in this work.

Conflict of interest

The authors declared that there is no conflict of interest.

References

Azmir, M.A., Ahsan, A.K., 2008. Investigation on glass/epoxy composite surfaces machined by abrasive water jet machining. Journal of Materials Processing Technology 198, 122–128.

Azmir, M.A., Ahsan, A.K., 2009. A study of abrasive water jet machining process on glass/epoxy composite laminate. Journal of Materials Processing Technology 209, 6168–6173.

Babu, N.M., Muthukrishnan, N., 2015. Investigation of multiple process parameters in abrasive water jet machining of tiles. Journal of the Chinese Institute of Engineers 38, 692–700.

Babu, M.N., Muthukrishnan, N., 2017. Exploration on Kerf-angle and surface roughness in abrasive waterjet machining using response surface method. International Journal of The Institution of Engineers Series C, 1–12.

Caydas, U., Hascalik, A., 2008. A study on surface roughness in abrasive water jet machining process using artificial neural networks and regression analysis method. Journal of Materials Processing Technology 202, 574–582.

Deb, K., 2005. Multi-objective optimization using evolutionary algorithms. Wiley India Pvt. Ltd, 2005.

Hasan, , Said, , Mustafa, N., 2008. The investigation of marble cutting parameters for energy consumption. International Journal of Mathematical Models and Methods in Applied Sciences 2, 462–472.

Irina Wong, M.M., Azmi, A.I., Lee1, C.C., Mansor, A.F., 2016. Kerf taper and delamination damage minimization of FRP hybrid composites under abrasive water-jet machining. The International Journal of Advanced Manufacturing Technology https://doi.org/10.1007/s00170-016-9669-y.

Jagadish, Bhowmik S., Ray, A., 2016. Prediction and optimization of process parameters of green composites in AWJM process using response surface methodology. The International Journal of Advanced Manufacturing Technology 87, 1359–1370.

Jain, N.K., Jain, V.K., Deb, K., 2007. Optimization of process parameters of mechanical type advanced machining processes using genetic algorithms. International Journal of Machine Tools and Manufacture 47, 900–919.

Jegaraj, J.J.R., Babu, N.R., 2007. A soft computing approach for controlling the quality of cut with abrasive water jet cutting system experiencing orifice and focusing tube wear. Journal of Materials Processing Technology 185, 217–227.

Karaboga, D., Basturk, B., 2008. On the performance of artificial bee colony (ABC) algorithm. Applied Soft Computing 8, 687–697.

Karakurt, I., Aydin, G., Aydiner, K., 2011. A machinability study of granite using abrasive waterjet cutting technology. Gazi University Journal of Science 24, 143–151.

Kechagias, J., Petropoulos, G., Vaxevanidis, N., 2012. Application of Taguchi design for quality characterization of abrasive water jet machining of TRIP sheet steels. International Journal of Advanced Manufacturing Technology 62, 635–643.

Liu, D., Huangn, C., Wang, J., Zhu, H., Yao, P., Liu, Z.W., 2014. Modeling and optimization of operating parameters for abrasive water jet turning alumina ceramics using response surface methodology combined with Box-Behnken design. Ceramics International 40, 7899–7908.

Luo, J., Liu, Q., Yang, Y., Li, X., Chen, M., Cao, W., 2017. An artificial bee colony algorithm for multi-objective optimization. Applied Soft Computing 50, 235–251.

Mali, A.Y., Pawar, P.J., 2017. Parametric optimization of abrasive water jet machining of glass fibre reinforced plastic composite using non-dominated sorting genetic algorithm-II. International Journal of Metaheuristics 6, 334–354.

Mukherjee, R., Goswami, D., Shankar, Chakraborty, 2013. Parametric optimization of Nd: YAG laser beam machining process using artificial bee colony algorithm. Journal of Industrial Engineering 2013, 1–15.

Orbabic, H., Junkar, M., 2008. Analysis of striation formation mechanism in abrasive water jet cutting. Wear 265, 821–830.

Pawar, P.J., Rao, R.V., 2012. Parameter optimization of machining processes using teaching–learning-based optimization algorithm. International Journal of Advanced Manufacturing Technology 67, 995–1006.

Rajkamal, S., Singh, D., 2017. Experimentation investigation of abrasive water jet machining parameters using Taguchi and Evolutionary optimization techniques. Swarm and Evolutionary Computation 32, 167–183.

Rao, R.V., Pawar, P.J., 2009. Modeling and optimization of process parameters of wire electric discharge machining. Journal of Engineering Manufacture 223, 1431–1440.

Rao, R.V., Rai, D.P., Balic, J., 2017. A multi-objective algorithm for optimization of modern machining processes. Engineering Applications of Artificial Intelligence 61, 103–125.

Selvan, C.P.M., Raju, N., Mohana, S., Sachidananda, H.K., 2012. Effects of process parameters on surface roughness in abrasive water jet cutting of aluminum. Frontiers of Mechanical Engineering 7, 439–444.

Srinivasu, D.S., Babu, R.N., 2008. A neuro-genetic approach for selection of process parameters in abrasive water jet cutting considering variation in diameter of focusing nozzle. Applied Soft Computing 8, 809–819.

Sumanta, S., Chakraborty, S., 2011. Parametric optimization of some non-traditional machining processes using artificial bee colony algorithm. Engineering Applications of Artificial Intelligence 24, 946–957.

Vundavilli, P.R., Parappagoudar, M.B., Kodali, S.P., Benguluri, S., 2012. Fuzzy logic-based expert system for prediction of depth of cut in abrasive water jet machining process. Knowledge-based Systems 27, 456–464.
Wang, Z., Li, Min, Dou, L., Li, Y., Zhao, Q, Li, J., 2015. A novel multi-objective artificial bee colony algorithm for multi-robot path planning. In: IEEE international conference on information and automation. pp. 481–486.
Yue, Z., Huang, C., Zhu, H., Wang, J., Yao, P., Liu, Z.W., 2014. Optimization of machining parameters in the abrasive water jet turning of alumina ceramic based on the response surface methodology. International Journal of Advanced Manufacturing Technology 71, 2107–2114.
Yusup, N., Sarkheyli, A., Zain, A.M., Hashim, S.Z.M., Ithnin, N., 2013. Estimation of optimal machining control parameters using artificial bee colony. Journal of Intelligent Manufacturing 25, 1463–1472.
Zain, A.M., Haron, H., Sharif, S., 2011. Estimation of the minimum machining performance in the abrasive water jet machining using integrated ANN-SA. Expert Systems with Applications 38, 8316–8326.
Zain, A.M., Haron, H., Sharif, S., 2011. Optimization of process parameters in the abrasive water jet machining using integrated SA–GA. Applied Soft Computing 11, 5350–5359.